TECHNICAL MEMORANDUM

491

A multivariate balance operator for variational ocean data assimilation

A. T. Weaver[1], C. Deltel[2], E. Machu[1], S. Ricci[1] and N. Daget[1]

Research Department

[1]Centre Européen de Recherche et de Formation Avancée en Calcul Scientifique, Toulouse, France
[2]Laboratoire d'Océanographie et du Climat - Expérimentation et Approches Numériques, Paris, France

To appear in *Q. J. R. Meteorol. Soc.*

April 2006

European Centre for Medium-Range Weather Forecasts
Europäisches Zentrum für mittelfristige Wettervorhersage
Centre européen pour les prévisions météorologiques à moyen terme

Series: ECMWF Technical Memoranda

A full list of ECMWF Publications can be found on our web site under:
http://www.ecmwf.int/publications/

Contact: library@ecmwf.int

European Centre for Medium-Range Weather Forecasts
Shinfield Park, Reading, RG2 9AX, England

Abstract

It is common in meteorological applications of variational assimilation to specify the error covariances of the model background state implicitly via a transformation from model space where variables are highly correlated to a control space where variables can be considered to be approximately uncorrelated. An important part of this transformation is a balance operator which effectively establishes the multivariate component of the error covariances. The use of this technique in ocean data assimilation is less common. This paper describes a balance operator that can be used in a variable transformation for oceanographic applications of three- and four-dimensional variational assimilation. The proposed balance operator has been implemented in an incremental variational data assimilation system for a global ocean general circulation model. Evidence that the balance operator can explain a significant percentage of background-error variance is presented. The multivariate analysis structures implied by the balance operator are illustrated using single observation experiments.

1 Introduction

The importance of the background-error covariances for determining the quality of analyses and forecasts is well known (Daley 1991). Specifying appropriate background-error covariances is a complex research problem which requires careful consideration of physical, statistical and computational issues. One important problem is how best to define the multivariate component of the background-error covariances. The multivariate component is responsible for transferring observational information between model variables and thus is critical for extracting information about unobserved variables from directly observed quantities. The problem of defining multivariate covariances is also intimately related to that of producing balanced initial conditions for initializing forecasts. In particular, improvements in the specification of multivariate covariances will usually translate into better dynamically balanced analyses and therefore can reduce, or even eliminate, the need for a separate 'initialization' procedure.

In oceanography, various approaches have been developed to introduce multivariate constraints in data assimilation systems. In some systems, they take the form of dynamical or physical constraints (e.g., geostrophic or temperature-salinity (T-S) relations) that are applied *a posteriori* to a statistically-generated univariate analysis (Burgers *et al.* 2002; Troccoli *et al.* 2002; Balmaseda 2004). While this generally leads to much better forecasts than if no constraints were applied at all, it does not make optimal use of multivariate information in defining the analysis itself and makes the assimilation of different data-types more difficult.

A more effective way of incorporating multivariate constraints in the data assimilation system is through the background error covariances. A popular method in oceanographic applications of sequential data assimilation schemes such as the Kalman filter is to compute the error covariances in a reduced-dimension subspace spanned by a limited number of three-dimensional (3D) empirical orthogonal functions (Testut *et al.* 2003) or a few members of an appropriately generated ensemble of ocean model states (Lermusiaux *et al.* 2000; Keppenne and Rienecker 2003). While reduced-space methods are capable of producing complex multivariate covariance structures, they have the disadvantage of restricting the analysis increment to lie only in the subspace spanned by the chosen basis vectors. Various localization techniques have been proposed to overcome this rank deficiency problem but unfortunately can be applied only at the expense of disrupting some of the attractive balance properties of the original covariances.

The specification of the multivariate component of the background-error covariances for variational ocean data assimilation has received much less attention. In ocean applications of four-dimensional variational assimilation (4D-Var), cross-variable correlations in the background errors are often neglected altogether (Bennett *et al.* 2000; Stammer *et al.* 2002; Weaver *et al.* 2003). This approximation is often justified by the fact that 4D-Var includes the ocean model (or a linearized version of the ocean model) as a constraint in the assimilation prob-

lem and so already contains a multivariate component. The validity of this approximation depends on several factors such as the length of the assimilation window, the choice of control variables, and the particular application. It is clearly a very poor approximation, however, in three-dimensional variational assimilation (3D-Var) which does not include the ocean model as a constraint. In general, a well-tuned multivariate background-error covariance model is beneficial to 4D-Var as well as 3D-Var.

This paper describes a very general method for incorporating multivariate constraints in variational ocean data assimilation. It extends the work of Ricci *et al.* (2005) who proposed a technique for incorporating T-S constraints in a 3D-Var system. The fundamental idea is to simplify the specification of the background-error covariances by designing a transformation from model state space, where variables are highly correlated, to another (control) space where variables can be considered approximately mutually uncorrelated. The basic technique is commonly used in meteorological applications of variational assimilation (Derber and Bouttier 1999; Cullen 2003) but has seen limited use in oceanography. In effect, the specification of the background-error covariances in model state space is transformed into one of defining a more general observation operator. An obvious advantage with this approach is that observation operators can be nonlinear whereas constraints that are included in traditional covariance (matrix) formulations are necessarily linear.

The paper is organized as follows. An outline of the general approach for modelling background-error covariances is given in section 2. Special attention is paid to some important practical issues concerning the implementation of the technique in incremental versions of 3D-Var and 4D-Var. Section 3 describes a multivariate balance operator that can be used in a control variable transformation for 3D-Var and 4D-Var applications with ocean general circulation models (OGCMs). The proposed balance operator has been implemented in a variational assimilation system for the OPA OGCM. Examples with this system are presented in section 4 to illustrate various properties of the balance operator. Conclusions are given in section 5. An appendix provides some mathematical details on the relationship between the balance operator and the multivariate component of the background-error covariance matrix.

2 An implicit representation of the background-error covariances

2.1 Formulation of the problem

The formulation of variational assimilation given by Derber and Wu (1998) provides a very general and convenient framework for representing background-error covariances in model state space. In their formulation, the variational analysis is defined by the minimization of a cost function of the form

$$J[\mathbf{v}] \;=\; \frac{1}{2}\,[\mathbf{v}-\mathbf{v}^b]^T\,[\mathbf{v}-\mathbf{v}^b] \;+\; \frac{1}{2}\,[G(\mathbf{v})-\mathbf{y}^o]^T\,\mathbf{R}^{-1}\,[G(\mathbf{v})-\mathbf{y}^o] \tag{1}$$

where $\mathbf{v}$ is the control (analysis) vector, $\mathbf{v}^b$ is the background estimate of the control vector, $\mathbf{y}^o$ is the vector of observations, $\mathbf{R}$ is an estimate of the observation error covariance matrix, including contributions from measurement and representativeness error, and G is a nonlinear operator that maps the control vector onto the space of the observation vector. The background-error covariance matrix of the control vector is assumed to be the identity matrix ($\mathbf{B}_{(\mathbf{v})} = \mathbf{I}$) as evident by the use of the canonical inner product for the background term in (1). In other words, background errors for $\mathbf{v}^b$ are assumed to be uncorrelated and to have unit variance. Clearly the control vector must be constructed carefully for this to be a reasonable assumption; e.g., it would be a very poor assumption if $\mathbf{v}$ were taken to be the model state vector. There are two advantages that result from this formulation where the background term takes on a very simple form. First, it generally improves the convergence properties of the minimization when the problem is solved with a conjugate gradient algorithm. For quadratic cost functions, this is often explained by a reduction in the condition number of the Hessian (Golub and Van

Loan 1996). Second, all constraints in the assimilation problem are now imposed through the nonlinear observation operator G, including multivariate and smoothness constraints that are used in conventional model-space (matrix) formulations of the background-error covariances. In particular, this opens the way for incorporating potentially more realistic (nonlinear) multivariate balance relationships in the analysis problem.

The control vector $\mathbf{v}$ is assumed to be related to the model state vector $\mathbf{x}$ through a transformation of the form

$$\mathbf{v} = U^{-1}(\mathbf{x}) \tag{2}$$

where U^{-1} is a block-matrix operator, with possibly nonlinear blocks, which is assumed to be square and invertible in the following. There is no complication if U is rectangular (i.e., if there are fewer control variables than state variables) but in this case U would only be invertible in a generalized sense. If the observations are distributed over a time window $t_0 \leq t_i \leq t_n$ then $\mathbf{x}$ can be interpreted, as in a conventional formulation of 4D-Var, as the initial state of the dynamical model used in G to propagate the model state forward to the observation times.[1]

Following Derber and Bouttier (1999), the operator U^{-1} can be split into three basic operators: a transformation K^{-1} that produces a set of approximately mutually uncorrelated variables by removing any known dynamical or physical balance relationships between model state variables; a diagonal matrix D^{-1} of normalization factors; and a roughening operator F^{-1} (the inverse of a smoothing operator) that acts separately on each of the uncorrelated variables. The change of variables (2) is needed to compute the background estimate, $\mathbf{v}^b$, of the control vector from the background estimate, $\mathbf{x}^b$, of the model state, while the inverse of the change of variables

$$\mathbf{x} = U(\mathbf{v}) = K(D(F(\mathbf{v}))) \tag{3}$$

is needed to evaluate the term $G(\mathbf{v})$ in the observation term. Equation (2) can be used to compute covariance statistics of the contrived control vector $\mathbf{v}$ from estimates of background error for the state vector $\mathbf{x}$. In practice, only a few aspects of the covariances (e.g., average variances) can be estimated reliably. From these estimates, the assumption that $\mathbf{B}_{(\mathbf{v})} \approx \mathbf{I}$ can be tested: if it is not well satisfied then either a new $\mathbf{B}_{(\mathbf{v})} \neq \mathbf{I}$ could be used to weight the background term in (1) or the parameters in the operators F, D and K could be recalibrated so that the approximation is better satisfied.

2.2 Incremental formulation

The incremental formulation (Courtier *et al.* 1994) provides a practical algorithm for approximately minimizing (1). The incremental algorithm is defined by the iterative minimization of a sequence, $k = 1, \ldots, K_o$, of quadratic cost functions

$$\begin{aligned} J^k[\delta\mathbf{v}^k] &= \frac{1}{2}\left[\delta\mathbf{v}^k - \mathbf{d}^{b,k}_{(\mathbf{v})}\right]^T \left[\delta\mathbf{v}^k - \mathbf{d}^{b,k}_{(\mathbf{v})}\right] \\ &+ \frac{1}{2}\left[\mathbf{G}^{k-1}\delta\mathbf{v}^k - \mathbf{d}^{o,k}\right]^T \mathbf{R}^{-1}\left[\mathbf{G}^{k-1}\delta\mathbf{v}^k - \mathbf{d}^{o,k}\right] \end{aligned} \tag{4}$$

where

$$\mathbf{d}^{b,k}_{(\mathbf{v})} = \mathbf{v}^b - \mathbf{v}^{k-1}, \tag{5}$$

$$\mathbf{d}^{o,k} = \mathbf{y}^o - G(\mathbf{v}^{k-1}) \tag{6}$$

[1] By interpreting $\mathbf{x}$ to be the initial conditions, the model and external forcing fi elds are tacitly assumed to be perfect. This assumption can be relaxed in the above formulation by considering $\mathbf{x}$ to contain model-error or external forcing terms in addition to the initial conditions.

is the innovation vector, $\mathbf{v}^{k-1}$ is a reference state, $\delta\mathbf{v}^k$ is an increment defined by $\mathbf{v}^k = \mathbf{v}^{k-1} + \delta\mathbf{v}^k$, and $\mathbf{G}^{k-1}$ is a linearized operator defined such that $G(\mathbf{v}^{k-1} + \delta\mathbf{v}^k) \approx G(\mathbf{v}^{k-1}) + \mathbf{G}^{k-1}\delta\mathbf{v}^k$ (when this equation is satisfied exactly, (4) is identical to (1)). The superscript $k-1$ indicates that $\mathbf{G}^{k-1}$ is the result of linearizing G about $\mathbf{v}^{k-1}$. The sequence $k = 1, ..., K_o$ are called outer iterations while the minimization iterations performed within each outer loop are called inner iterations. Equations (5) and (6) are the effective "background" and "observation" vectors for the inner loop minimization. In practice, it is customary to set $\mathbf{v}^0 = \mathbf{v}^b$ and to choose $\mathbf{v}^{k-1}$, for $k = 2, ..., K_o$, to be the solution obtained at the end of the previous outer loop. The minimum of (4) after the K_o-th outer iteration defines the analysis increment, $\delta\mathbf{v}^a = \delta\mathbf{v}^{K_o}$. The analysis in model space is then given by $\mathbf{x}^a = U(\mathbf{v}^a)$ where $\mathbf{v}^a = \mathbf{v}^{K_o-1} + \delta\mathbf{v}^a$.

The nonlinear transformation (3) is needed on each outer iteration to evaluate the term $G(\mathbf{v}^{k-1})$ in (4). Through successive linearizations about $\mathbf{v}^l$, $l = 0, ..., k-2$, this transformation can be approximated by

$$\mathbf{x}^{k-1} = U(\mathbf{v}^{k-1}) \approx U(\mathbf{v}^0) + \sum_{l=1}^{k-1} \mathbf{U}^{l-1}\delta\mathbf{v}^l. \tag{7}$$

By choosing $\mathbf{v}^0 = \mathbf{v}^b$, the first term on the right-hand-side of (7) becomes $U(\mathbf{v}^0) = U(\mathbf{v}^b) \equiv \mathbf{x}^b$. Equation (7) then implies that $\mathbf{x}^{k-1}$ can be approximated as the sum of the model-space background state and the model-space increments estimated using the inverse of the *linearized* change of variables. A further consequence of choosing $\mathbf{v}^0 = \mathbf{v}^b$ is that the difference vector (5) can be written as minus the sum of the increments generated from previous outer iterations:

$$\mathbf{d}^{b,k}_{(\mathbf{v})} = \mathbf{v}^0 - \mathbf{v}^{k-1} = -\sum_{l=1}^{k-1} \delta\mathbf{v}^l. \tag{8}$$

Equation (8) together with the approximation (7) allow us to eliminate the explicit dependence of (4) on $\mathbf{v}^{k-1}$ and thus to iterate the incremental minimization algorithm without the need to perform either the nonlinear transformation (2) or its inverse (3) (only the linearized transformations are required).

To complete the evaluation of $G(\mathbf{v}^{k-1})$, $\mathbf{x}^{k-1}$ must be propagated to the observation times using the model operator and then transformed to the observed quantities using the observation operator. The linearized counterpart of this operator is required to evaluate $\mathbf{G}^{k-1}\delta\mathbf{v}^k$ in (4). As discussed in Weaver *et al.* (2003), 3D-Var and 4D-Var can be distinguished by the type of linear model that is used to evolve the increments between observation times. In 3D-Var the increments are persisted whereas in 4D-Var they are evolved by a dynamical model that closely approximates the tangent-linear model. By distinguishing 3D-Var and 4D-Var at the incremental level, they can be viewed as two different algorithms for approximately solving the same 4D assimilation problem described by the nonquadratic cost function (1).

2.3 Diagnosing the effective background-error covariance matrix

Although the background-error covariance matrix in model space has not been defined explicitly, its effective form on a given outer iteration can be easily diagnosed by transforming the background term in (4) into model space using the linearized change of variables $\delta\mathbf{v}^k = \left(\mathbf{U}^{k-1}\right)^{-1}\delta\mathbf{x}^k$ and its inverse $\delta\mathbf{x}^k = \mathbf{U}^{k-1}\delta\mathbf{v}^k$. This yields

$$J^k_b = \frac{1}{2}\left[\delta\mathbf{x}^k - \mathbf{d}^{b,k}_{(\mathbf{x})}\right]^T \left(\mathbf{B}^k_{(\mathbf{x})}\right)^{-1} \left[\delta\mathbf{x}^k - \mathbf{d}^{b,k}_{(\mathbf{x})}\right] \tag{9}$$

where

$$\mathbf{B}^k_{(\mathbf{x})} = \underbrace{\mathbf{K}^{k-1}\,\mathbf{D}^{k-1}_{(\widehat{\mathbf{x}})}\,\mathbf{F}^{k-1}}_{\mathbf{U}^{k-1}} \underbrace{\mathbf{F}^{k-1^T}\,\mathbf{D}^{k-1^T}_{(\widehat{\mathbf{x}})}\mathbf{K}^{k-1^T}}_{\mathbf{U}^{k-1^T}}, \tag{10}$$

and $\mathbf{d}^{b,k}_{(\mathbf{x})} = \mathbf{U}^{k-1}\mathbf{d}^{b,k}_{(\mathbf{v})}$. Equation (10) corresponds to the model background-error covariance matrix on the k-th outer iteration. Since $\mathbf{B}^{k}_{(\mathbf{x})}$ depends, in general, on the linearization state $\mathbf{x}^{k-1}$, it may vary from one outer iteration to the next. In this way, the outer iterations provide an adaptive mechanism for modifying the background-error covariance model during the course of minimization. The background-error covariance matrix $\mathbf{B}^{K_o}_{(\mathbf{x})}$ used on the final outer iteration K_o would be the effective covariance matrix used for the analysis. Note that in 4D-Var, $\mathbf{B}^{K_o}_{(\mathbf{x})}$ would be evolved (implicitly) within the assimilation window through the action of the linearized dynamical model and its adjoint (Courtier *et al.* 1994). In 3D-Var, on the other hand, $\mathbf{B}^{K_o}_{(\mathbf{x})}$ would be fixed within the assimilation window, although, as in 4D-Var, it may vary from one assimilation cycle to the next through its dependence on the background state.

Equation (10) provides a valuable statistical interpretation of the control variable transformation. The product $\mathbf{F}^{k-1}(\mathbf{F}^{k-1})^T$ of the linearized smoothing matrix and its transpose can be interpreted as a correlation matrix, provided that care has been taken to normalize the matrix so that the diagonal elements are all equal to one. The correlations in $\mathbf{F}^{k-1}(\mathbf{F}^{k-1})^T$ correspond to those of the errors of the transformed background variables $\widehat{\mathbf{x}}^b = K^{-1}(\mathbf{x}^b)$, not to the error correlations of $\mathbf{x}^b$ itself. By construction, cross-correlations between these variables are neglected so that $\mathbf{F}^{k-1}(\mathbf{F}^{k-1})^T$ is block-diagonal (univariate), where each block corresponds to the auto-correlation matrix for each variable in $\widehat{\mathbf{x}}^b$. While the cross-correlations will never be exactly zero in practice, the intent is that with an astutely chosen K^{-1} operator, they can be made sufficiently small so that neglecting them is an acceptable assumption.

The diagonal matrix $\mathbf{D}^{k-1}_{(\widehat{\mathbf{x}})}$ in (10) contains estimates of the standard deviations of the errors in $\widehat{\mathbf{x}}^b$. In meteorology, it is typical to estimate the standard deviations (and parameters of the correlation model) from a suitably constructed ensemble of forecast differences (Parrish and Derber 1992; Buehner 2005). To estimate statistics of the control variables, the forecasts must first be transformed into $\widehat{\mathbf{x}}$-space using K^{-1} or, as an approximation, the forecast differences can be transformed directly using the linearized balance operator $\mathbf{K}^{k-1}$. In (10), $\mathbf{K}^{k-1}$ couples the different model variables and thus establishes the multivariate component of the background-error covariances in $\mathbf{x}$-space (Derber and Bouttier 1999). The remainder of this article is devoted to the specification of a balance operator for ocean data assimilation. The problems of estimating background-error covariances and deriving efficient and general smoothing algorithms for representing background-error correlations are both very important but a proper discussion of these issues goes beyond the scope of this paper.

3 A balance operator for ocean state variables

3.1 General formulation

The variables comprising the model state vector are assumed to be potential temperature T, salinity S, sea surface height (SSH) η, and the components of the horizontal velocity vector $\mathbf{u}^h = (u,v)^T$[2]. These variables correspond to the standard prognostic variables in a free-surface, hydrostatic OGCM. In this section, an operator K^{-1} is developed which can be used to transform $\mathbf{x} = (T,S,\eta,\mathbf{u}^h)^T$ into a vector $\widehat{\mathbf{x}} = (T,S_U,\eta_U,\mathbf{u}^h_U)^T$ whose elements T, S_U, η_U and $\mathbf{u}^h_U = (u_U,v_U)^T$ can be considered to be approximately mutually uncorrelated. This can be achieved by separating the state variables into *unbalanced* and *balanced* components (Derber and Bouttier 1999), except for one variable, taken here to be T, which is treated in totality and used as the starting point to establish the balanced part of the other variables. The other elements S_U, η_U etc. of $\widehat{\mathbf{x}}$ represent the unbalanced part of that particular variable.

[2] A superscript T will continue to denote the transpose of a matrix or vector and should not be confused with the potential temperature variable T.

The balance relationships used to define $\mathbf{x} = K(\widehat{\mathbf{x}})$ are described in detail in the next section. Symbolically, the balance operator can be summarized by the sequence of equations

$$\begin{array}{rclcrclcrcl} T & = & T & & & & & & & & \\ S & = & K_{ST}(T) & + & S_U & = & S_B & + & S_U \\ \eta & = & K_{\eta\rho}(\rho) & + & \eta_U & = & \eta_B & + & \eta_U \\ u & = & K_{up}(p) & + & u_U & = & u_B & + & u_U \\ v & = & K_{vp}(p) & + & v_U & = & v_B & + & v_U \end{array} \tag{11}$$

where

$$\begin{array}{rcl} \rho & = & K_{\rho TS}(T,S) \\ p & = & K_{p\rho}(\rho) + K_{p\eta}(\eta) \end{array} \tag{12}$$

are diagnostic quantities corresponding to density and pressure, respectively, and K_{xy} represents the transformation from the variable(s) y to x. The variables with a subscript B on the right-hand-side of (11) represent the balanced component of those variables. The lower block-triangular structure of the balance operator (11) implies that a balanced variable can be a function of the variables preceding it in the sequence but will be independent of the variables following it in the sequence. It also allows the inverse balance operator K^{-1} to be obtained trivially from the sequence of equations

$$\begin{array}{rcrcl} T & = & T & & \\ S_U & = & S & - & S_B \\ \eta_U & = & \eta & - & \eta_B \\ u_U & = & u & - & u_B \\ v_U & = & v & - & v_B. \end{array} \tag{13}$$

A linearized version of $\mathbf{x} = K(\widehat{\mathbf{x}})$ is required for the incremental formulation. According to (7), the linearized balance equation can be approximated as

$$\mathbf{x}^{k-1} \approx \mathbf{x}^b + \sum_{l=1}^{k-1} \delta\mathbf{x}^l \tag{14}$$

where $\delta\mathbf{x}^l = \mathbf{K}^{l-1}\,\delta\widehat{\mathbf{x}}^l$. This approximation is very convenient since it eliminates the need to specify the nonlinear version of the balance operator (it is implicit in $\mathbf{x}^b$). It is used in the rest of this section and in the illustrations presented in section 4. It can be expected to be a good approximation when the balance operator is weakly nonlinear.

From (11) and (12), the linear balance equations for the increment can be written in the general form

$$\begin{array}{rclcrclcrcl} \delta T^k & = & \delta T^k & & & & & & & & \\ \delta S^k & = & \mathbf{K}_{ST}^{k-1}\,\delta T^k & + & \delta S_U^k & = & \delta S_B^k & + & \delta S_U^k \\ \delta \eta^k & = & \mathbf{K}_{\eta\rho}\,\delta\rho^k & + & \delta \eta_U^k & = & \delta \eta_B^k & + & \delta \eta_U^k \\ \delta u^k & = & \mathbf{K}_{up}\,\delta p^k & + & \delta u_U^k & = & \delta u_B^k & + & \delta u_U^k \\ \delta v^k & = & \mathbf{K}_{vp}\,\delta p^k & + & \delta v_U^k & = & \delta v_B^k & + & \delta v_U^k \end{array} \tag{15}$$

where

$$\begin{array}{rclcl} \delta\rho^k & = & \mathbf{K}_{\rho T}^{k-1}\,\delta T^k & + & \mathbf{K}_{\rho S}^{k-1}\,\delta S^k \\ \delta p^k & = & \mathbf{K}_{p\rho}\,\delta\rho^k & + & \mathbf{K}_{p\eta}\,\delta\eta^k. \end{array} \tag{16}$$

As described below, nonlinear operators are used for the salinity balance K_{ST} and the density balance $K_{\rho TS}$. All the other balance operators are linear and thus independent of the linearization state $\mathbf{x}^{k-1}$. This has been made clear in (15) by omitting the superscript $k-1$ from those matrix operators.

3.2 A set of linearized balance relationships

Temperature plays an important role in the balance formulation since is used to compute all, or a significant part of, the balanced component of the other variables. The relationship between temperature (T) and salinity (S) is complex and traditionally determined empirically from scatter plots of historical T and S data. Han *et al.* (2004) propose fitting a high-order polynomial function to T-S diagrams in order to determine an explicit S(T) relationship. This procedure can work reasonably well in some data-rich regions such as the western tropical Pacific Ocean, as illustrated by Han *et al.* (2004). Using a somewhat different formulation to the one presented here, Han *et al.* (2004) then go on to show how such an S(T) relationship, together with an estimate of the uncertainty in this relationship, can be used to correct salinity from temperature data within a variational assimilation framework.

Troccoli and Haines (1999) propose an alternative and simpler method for adjusting salinity when only temperature information is available. Their approach is designed to preserve the T-S properties of the background state by making vertical displacements of the local background salinity field in response to changes to the local background temperature field produced by the assimilation of temperature data. The attractive features of their method are that it can be applied in a global system, it allows for state-dependency in the T-S relation, and it does not require any prior statistical analysis of an observational database.

Ricci *et al.* (2005) describe a simple variant of the Troccoli and Haines (1999) scheme for implementation within a linear balance operator. In their study, balanced salinity increments are defined by

$$\delta S_B^k \;=\; \gamma^{k-1} \left.\frac{\partial S}{\partial z}\right|_{S=S^{k-1}} \left.\frac{\partial z}{\partial T}\right|_{T=T^{k-1}} \delta T^k \tag{17}$$

where $\gamma^{k-1} = \gamma^{k-1}(T^{k-1}, S^{k-1}, u^{k-1}, v^{k-1})$ is a coefficient that is set to either zero or one, depending on various conditions in the reference state. For example, to take into account the weak correlation between temperature and salinity in well-mixed regions, γ^{k-1} is set to zero at grid points where the reference vertical mixing coefficient is large, such as in the ocean mixed layer. When $\gamma^{k-1} = 0$, δS^k is entirely described by its unbalanced component δS_U. To avoid a discontinuity in the balance at the base of the mixed layer, δS_B^k is smoothly reduced to zero at the surface from its non-zero value just below the mixed layer. The vertical derivatives in (17) are used to estimate the local derivative of the background T-S relation and can be computed using finite differences or a cubic spline. In practice, it has been found desirable to apply a horizontal smoothing operator (e.g., the one used in $\mathbf{F}^{k-1}$) to the balance coefficient in (17) in order to avoid generating noisy salinity increments. The impact of the T-S balance has been evaluated in detail by Ricci *et al.* (2005) in a multi-annual cycled 3D-Var experiment for the tropical Pacific Ocean. When assimilating temperature data alone, they showed that the constraint can have a significant positive impact on velocity as well as salinity compared to a 3D-Var analysis in which no T-S constraint is applied. Notice that, as the T-S constraint is dependent on the reference state, it can evolve both during the course of minimization (via outer iterations) and from one assimilation cycle to the next.

Density can be computed from potential temperature and salinity using a nonlinear equation of state (e.g., McDougall *et al.* 2003). The (balanced) density increment can be defined by linearizing the equation of state about the reference state:

$$\delta\rho^k \;=\; \rho_0 \left(-\alpha^{k-1}\delta T^k \;+\; \beta^{k-1}\delta S^k \right) \tag{18}$$

where $\alpha^{k-1} = (1/\rho_0)\,\partial\rho/\partial T|_{S=S^{k-1},T=T^{k-1}}$ and $\beta^{k-1} = (1/\rho_0)\,\partial\rho/\partial S|_{S=S^{k-1},T=T^{k-1}}$ are thermal and saline expansion coefficients, respectively, and ρ_0 is a constant reference density.

SSH can be computed diagnostically as a function of the state variables T, S and $\mathbf{u}^h$ by filtering out nonstationary contributions to SSH (e.g., from high frequency gravity waves) using the rigid-lid approximation (Fukumori

et al. 1998). Furthermore, for flow regimes where the Rossby number is weak (regimes close to geostrophic balance), contributions to SSH from advection, dissipation, and surface forcing can be neglected. The resulting equation approximates SSH as the sum of two terms: a baroclinic term that depends on density and a barotropic term that depends on the depth-integrated transport. For the global model used in the illustrations in the next section, Ferry (2003) has demonstrated that SSH variability is indeed dominated by its baroclinic and barotropic components, except in coastal regions where the contribution from surface forcing can be important. In the following, the baroclinic and barotropic contributions to SSH are taken to be the balanced and unbalanced parts of SSH, respectively.

The balanced (baroclinic) component can be estimated by computing the dynamic height at the surface $z = 0$ relative to a reference depth z_{ref}:

$$\delta\eta_B^k \;=\; -\int_{z'=z_{ref}}^{0} \left(\delta\rho^k(z')\,/\,\rho_0\right) dz'. \tag{19}$$

($z_{ref} = 1500\,\mathrm{m}$ in the examples in section 4). Equation (19) is only an approximation of the baroclinic part of (the increment of) SSH. The complete expression involves the solution of an elliptic equation (Fukumori *et al.* 1998):

$$\nabla\cdot H\nabla\delta\eta_B^k \;=\; -\nabla\cdot\int_{z=-H}^{0}\int_{z'=z}^{0} \left(\nabla\delta\rho^k(z')\,/\,\rho_0\right) dz'\,dz \tag{20}$$

where $z = -H(\lambda,\phi)$ is the total ocean depth, λ is longitude, ϕ is latitude, and ∇ and $\nabla\cdot$ are the horizontal gradient and divergence operators, respectively. Equation (20) takes into account variations in topography and is independent of a reference depth, and therefore would be more accurate than (19) in regions where bathymetry is important or where the ocean is shallow. For this study, however, the simpler equation (19) has been adopted.

The balanced pressure increment at any depth z can be computed by integrating the hydrostatic equation from z to the surface:

$$\delta p^k(z) \;=\; \int_{z'=z}^{0} \delta\rho^k(z')\,g\,dz' \;+\; \rho_0\,g\,(\delta\eta_B^k + \delta\eta_U^k) \tag{21}$$

where the second term on the right-hand-side of (21) is the pressure exerted by the surface elevation, $\delta p^k(0) = \rho_0\,g\,\delta\eta^k$ with $\delta\eta^k$ given by (15). Substituting (19) in (21) and reversing the order of integration of the first term on the right-hand-side of (21) leads to

$$\delta p^k(z) \;=\; -\int_{z'=z_{ref}}^{z} \delta\rho^k(z')\,g\,dz' \;+\; \rho_0\,g\,\delta\eta_U^k. \tag{22}$$

Away from the equator, the balanced part of the horizontal velocity components $(\delta u_B^k, \delta v_B^k)$ is assumed to be in geostrophic balance; i.e., proportional to the horizontal gradient of (22) divided by the Coriolis parameter f. The horizontal gradient of the first term in (22) is associated with a *baroclinic* geostrophic velocity, while that of the second term is associated with a *barotropic* geostrophic velocity. The ageostrophic components of the velocity increment are assumed to be associated with the unbalanced components $(\delta u_U^k, \delta v_U^k)$.

Special treatment of the geostrophic velocity balance is required near the equator where $f \to 0$. There, the zonal component δu_B^k is taken to be geostrophically balanced while the meridional component δv_B^k is reduced to zero. Geostrophic balance for δu_B^k is computed near the equator using a β-plane geostrophic approximation (Lagerloef *et al.* 1999), which involves the meridional derivative of the geostrophic equation. For this balance to exist, the meridional pressure gradient must exactly vanish at the equator so that the standard (undifferentiated) form

of the geostrophic equation is satisfied when $f = 0$. Picaut and Tournier (1991) suggest adding a latitudinally-dependent correction term to the pressure field in order to force a zero meridional gradient at the equator while leaving the meridional curvature of the original pressure field, and hence the estimate of the zonal geostrophic current via the β-plane approximation, unaltered. A similar technique is adopted here. The correction term effectively filters out all flows with anti-symmetric pressure structures about the equator. An important exception is an equatorial Kelvin wave, which is associated with a strictly zonal current in geostrophic balance and is thus described by the proposed velocity balance on the equator.

To allow for a smooth transition between the equatorial (β-plane) geostrophic velocity and the standard (f-plane) geostrophic velocity away from the equator, weighting functions $W_\beta = \exp(-\phi^2/2L_\beta^2)$ and $W_f = 1 - W_\beta$ are introduced, where L_β is a length scale whose size is of the order of the equatorial Rossby radius of deformation (Lagerloef *et al.* 1999). At the equator, $W_\beta = 1$ and $W_f = 0$, while far away from the equator, $W_\beta \approx 0$ and $W_f \approx 1$. Experimental evidence is given by Lagerloef *et al.* (1999) to justify the Gaussian form for the weighting function. The complete expression for the increments of the balanced velocity components in spherical coordinates is then given by

$$\delta u_B^k = -\frac{1}{\rho_0}\left(\frac{W_f}{f} + \frac{W_\beta}{\beta}\frac{1}{a}\frac{\partial}{\partial\phi}\right)\frac{1}{a}\frac{\partial\delta\widetilde{p}^k}{\partial\phi} \tag{23}$$

$$\delta v_B^k = \frac{1}{\rho_0}\frac{W_f}{f}\frac{1}{a\cos\phi}\frac{\partial\delta\widetilde{p}^k}{\partial\lambda} \tag{24}$$

where $\beta = \partial f/\partial(a\phi)$, and a is the radius of the Earth. To simplify the β-plane approximation, the differentiated term involving the product $f\,\partial\delta u_B^k/\partial(a\phi)$ has been neglected in (23). This term can be expected to be relatively small near the equator where $f \approx 0$. Following Picaut and Tournier (1991), the modified pressure increment in (23) and (24) is defined by

$$\delta\widetilde{p}^k = \delta p^k - \phi\left(\frac{\partial\delta p^k}{\partial\phi}\right)_{\phi=0}\exp(-\phi^2/2L_p^2) \tag{25}$$

where the second term on the right-hand-side (25) corresponds to the pressure correction factor. The correction term does not affect (24), is negligible far from the equator, and satisfies both the β-plane constraint $\left(\partial^2\delta\widetilde{p}^k/\partial\phi^2\right)_{\phi=0} = \left(\partial^2\delta p^k/\partial\phi^2\right)_{\phi=0}$ and the necessary condition for geostrophic balance at the equator, $\left(\partial\delta\widetilde{p}^k/\partial\phi\right)_{\phi=0} = 0$. The length scales L_p in the correction term and L_β in the weighting functions are taken to be equal and set to 1.55° as in Lagerloef *et al.* (1999).

4 Illustrations

The balance operator described in the previous section has been implemented in a 3D-Var/4D-Var system (Weaver *et al.* 2003) for a global, free-surface version of the OPA OGCM (Madec *et al.* 1998; Roullet and Madec 2000). The system has been exploited within the framework of the European ENACT project (see http://www.ecmwf.int/research/EU_projects/ENACT) to produce global ocean reanalyses using historical temperature and salinity data (Ingleby and Huddleston 2005) and surface forcing fields from the ERA40 atmospheric reanalysis (Uppala *et al.* 2005). It is beyond the scope of this paper to provide a thorough description of the system and assessment of the reanalyses. Only certain aspects of the system concerning the balance operator and background-error covariance formulation are discussed and illustrated here.

4.1 Evidence of balance in ocean background errors

The balance operator can be considered effective if the variance of background error of the balanced variables explains a substantial part of the variance of background error of the full variables. If this is not the case then the balance operator would provide little useful information for the analysis. Since actual background error is unknown, a suitable proxy must be defined in order to estimate its statistical properties. Here, background error is approximated as the difference between the background state $(\mathbf{x}^b(t_n))$ and the reference state $(\mathbf{x}^K(t_n))$ at the end of an assimilation window. The two states will differ since the background state over the window $t_0 \leq t_i \leq t_n$ is obtained by forcing the model with the atmospheric fluxes only, whereas the reference state is obtained by assimilating data over $t_0 \leq t_i \leq t_n$ in addition to applying the surface forcing. This approach is analogous to the so-called NMC method used in meteorology to estimate background-error statistics (Parrish and Derber 1992). Berre *et al.* (2005) discuss the conditions for which the NMC method is a good approximation to true forecast error.

A set of 328 background-minus-reference state differences has been obtained by cycling the 3D-Var system over the 9-year period 1993–2001 using a 10-day window. The inverse of the linearized balance operator was then applied to each of these difference fields in order to retrieve the unbalanced components. From the average variance, $\sigma^2_{\mathbf{x}}$, of the full fields and the average variance, $\sigma^2_{\mathbf{x}_U}$, of the unbalanced fields, the percentage ratio of explained variance $r = (1 - \sigma^2_{\mathbf{x}_U}/\sigma^2_{\mathbf{x}}) \times 100\%$ was computed. For the global average, r is 37% for salinity, 94% for SSH, and 70% and 44% for the zonal and meridional components of velocity, respectively. Errors computed using the NMC method were artificially small in regions poleward of 65°N/S and below 1000m since no data were assimilated there. Those regions were thus excluded from the global average. In so far as the NMC method provides a reasonable representation of background errors, these results suggest that the proposed balance operator can explain a substantial amount of actual background-error variance.

The percentage variance ratio has also been computed as a function of depth from the horizontally-averaged variances in each model level, and as a function of latitude from the zonally- and depth-averaged variances. The results are displayed in Figs. 1a and b. For salinity (solid curve), r is largest (up to 80%) below the level of the mean thermocline (below 200m), and reduces gradually to zero between 200m and the surface (Fig. 1a). The small value of r close to the surface is understandable since the salinity balance is deliberately reduced in regions of strong mixing such as the surface mixed layer. Figure 1b suggests that the salinity balance is most effective in the subtropical gyre regions (between 10°N(S) and 30°N(S)). For the u-component of velocity (dashed curve), r is relatively uniform with depth, with values between 60% and 70%. The explained variance is about 20% to 40% smaller for v than u, and decreases more rapidly with depth. The velocity balance for the u-component is effective at all latitudes, even at the equator where it explains about 50% of the variance. The value of r for the v-component (dotted curve) is, as expected, small near the equator where the weight given to the geostrophic equation for v is reduced to zero (Eq. 24), but is comparable to the value of r for the u-component poleward of about 10°N/S. The SSH balance is particularly effective and explains over 90% of the variance within 40° of the equator (dashed-dotted curve). At mid- and high latitudes, the barotropic (unbalanced) component is known to be important, which probably explains the reduction in r in this region.

It is worth noting that if the balanced and unbalanced fields were truly independent then $\sigma^2_{\mathbf{x}} = \sigma^2_{\mathbf{x}_B} + \sigma^2_{\mathbf{x}_U}$, where $\sigma^2_{\mathbf{x}_B}$ denotes the variance of the balanced field. The percentage variance ratio r would thus be equivalent to $\widehat{r} = (\sigma^2_{\mathbf{x}_B}/\sigma^2_{\mathbf{x}}) \times 100\%$. Comparing $\widehat{r}$ with r would then provide a measure of the validity of the assumption that the two fields are approximately uncorrelated. In particular, comparing Figs. 1a and b with the equivalent figures for $\widehat{r}$ (not shown) illustrates that r and $\widehat{r}$ do have similar structure and amplitude for all fields, except for u and v for which there is a tendency for $\widehat{r}$ to increase with depth rather than decrease with depth as in Fig. 1a. The reasons for this discrepancy are not known at present but will need to be explored in future work.

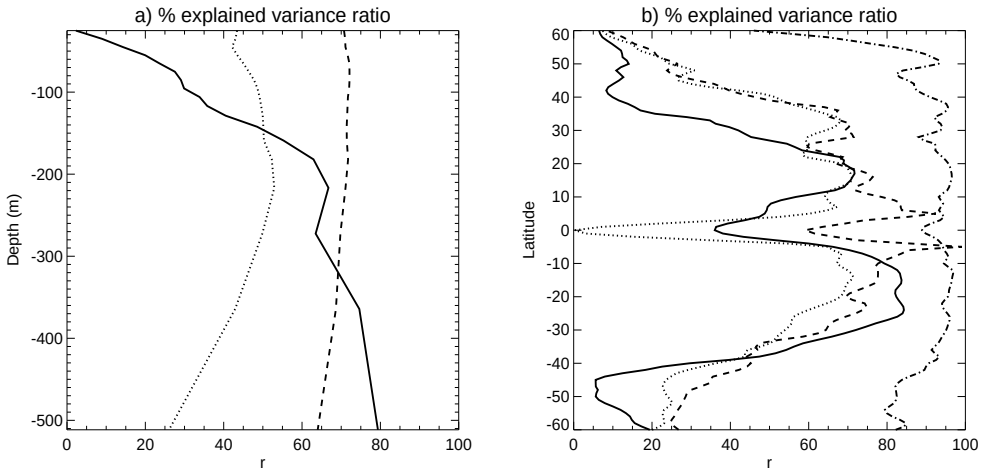

Figure 1: The percentage ratio (r) of background-error variance explained by the balanced part of salinity (solid curve), SSH (dashed-dotted curve), the u-component of velocity (dashed curve) and the v-component of velocity (dotted curve). a) r computed from horizontally-averaged variances and plotted as a function of depth; b) r computed from zonally- and depth-averaged variances and plotted as a function of latitude. Background errors have been estimated from a set of 329 background-minus-reference state differences.

4.2 Single observation experiments with 3D-Var and 4D-Var

The multivariate properties of the background-error formulation are most clearly illustrated using single observation experiments. A mathematical demonstration of this point is given in Appendix A. For simplicity, the unbalanced components of salinity, SSH and velocity are ignored (they are assumed to have zero error variance) so that only the univariate T covariances need to be specified. In other words, the balance operator is applied as a strong constraint (Lorenc 2003). This is sufficient to illustrate basic properties of the balance operator which is the objective here. For practical applications, however, it would be better to apply the balance operator as a weak constraint by prescribing a non-zero covariance to the unbalanced components, provided reasonable estimates of these covariances can be computed (e.g., using ensemble methods).

The univariate 3D smoothing operator for T is defined as the product of a 1D and 2D anisotropic diffusion operator (Weaver and Courtier 2001). The resulting correlation structures are approximately Gaussian. The parameters of the 3D diffusion operator are the same as those used for the T-T correlations in the study of Weaver *et al.* (2003), except for the vertical correlation scales which have been slightly reduced here. The error variances, $(\sigma_T^k)^2$, for T have been made dependent on the vertical gradient of the reference T field in order to focus the largest errors at the level of the thermocline where thermal variability is greatest. Weaver *et al.* (2003) illustrate how this simple parameterisation of the background T errors can account for some of the dynamical effects implicit in a Kalman filter. A similar parameterisation is used in the operational ocean data assimilation systems at the National Centers for Environmental Prediction (Behringer *et al.* 1998) and European Centre for Medium-Range Weather Forecasts (Alves *et al.* 2004). To avoid prescribing unrealistically small variances in the mixed layer and deep ocean where vertical T gradients are small, the parameterisation is modified so that

$$\sigma_T^k = \begin{cases} \max\left\{\tilde{\sigma}_T^k,\ \sigma_T^{ml}\right\} & \text{in the mixed layer,} \\ \max\left\{\tilde{\sigma}_T^k,\ \sigma_T^{do}\right\} & \text{below the mixed layer,} \end{cases} \tag{26}$$

where

$$\tilde{\sigma}_T^k = \min\left\{\left|\left(\partial T/\partial z|_{T=T^{k-1}}\right)\ \delta z\right|,\ \sigma_T^{max}\right\}, \tag{27}$$

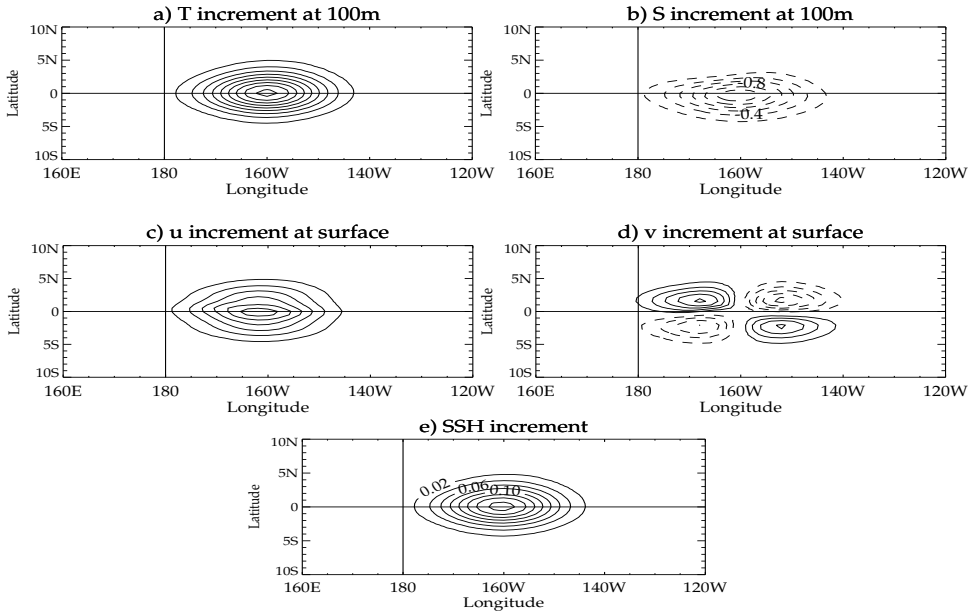

Figure 2: Horizontal sections of the analysis increments for a) temperature, b) salinity, c) zonal velocity, d) meridional velocity, and e) SSH generated by the 3D-Var assimilation of a single temperature observation (positive innovation) located at a depth of 100m on the equator in the central Pacific. The contour interval is 2.0 K in a), 0.2 psu in b), 0.1 m/s in c), 0.01 m/s in d), and 0.02 m in e). The fields have been multiplied by a factor 100. Solid (dashed) contours indicate positive (negative) values.

σ_T^{max} being the maximum-allowed value of σ_T^k, δz a vertical scale, and σ_T^{ml} and σ_T^{do} lower bounds in the mixed layer and deep ocean, respectively. The specification of σ_T^k is thus transformed into one of choosing appropriate values for these parameters. For the examples presented here, $\sigma_T^{max} = 1.5$ K, $\delta z = 10$ m, $\sigma_T^{ml} = 0.5$ K, and $\sigma_T^{do} = 0.07$ K.

In the first example, the impact of a single T observation in 3D-Var is considered. For this special case, the analysis of the T field depends entirely on the univariate T covariances (it is independent of the balance operator) and the analysis increments for the other variables are independent of the univariate covariances of their unbalanced component. Those increments could be obtained *a posteriori* by applying the linearized balance operator directly to the analyzed T increment. This point is clarified in the appendix. Figure 2 shows the 3D-Var analysis increment for a single T observation chosen to be 1 K warmer than the background T value, and located in the thermocline (100m) on the equator in the central Pacific (160°W). The observation-error variance has been set to $(1.0\ \mathrm{K})^2$. These increments are proportional to the implicitly defined background-error covariances with T at the observation point ($K_o = 1$ in all experiments). The structures are physically sensible. The positive T anomaly in the subsurface (Fig. 2a) is associated with an elevated SSH (Fig. 2e) and a geostrophic current at the surface with an eastward zonal component that is symmetric about the equator (Figs. 2c) and a meridional component that is asymmetric about the equator (Figs. 2d). The dependence of the T-S balance and the T error variances on the reference state can lead to an anisotropic response in the T and S increments. To avoid generating noisy increments, both the T-S balance coefficients and σ_T^b were smoothed in each level using the horizontal diffusion operator in $\mathbf{F}^{k-1}$.

The previous example does not illustrate the full potential of the balance operator for exploiting different observation types in the assimilation process. When information about state variables other than T is assimilated, the analysis results from a generally complex interaction between the balance operator, its adjoint and the covariance statistics of the uncorrelated variables. For example, a SSH observation would provide direct information

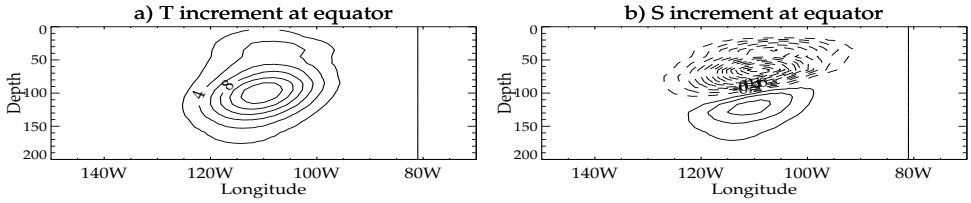

Figure 3: Vertical cross section at the equator of the analysis increments for a) temperature and b) salinity generated by the 3D-Var assimilation of a single SSH observation (positive innovation) located on the equator in the central Pacific. The contour interval is 2.0 K in a), and 0.1 psu in b). The fields have been multiplied by a factor 100. Solid (dashed) contours indicate positive (negative) values.

on SSH as well as indirect information on T and S via the dynamic height relation (19). In this case, the covariances for the unbalanced components of S and SSH, as well as those for T, would influence the analysis, and the adjoint of the balance operator would be required in the minimization process to map gradient information from SSH into gradient information for the other fields (see Appendix A).

Figure 3 shows a zonal-vertical section at the equator of the T increment (Fig. 3a) and S increment (Fig. 3b) generated by the 3D-Var assimilation of a single SSH observation, chosen to be 5 cm higher than the background SSH, on the equator in the eastern Pacific (110°W). The observation-error variance has been set to $(0.5\,\mathrm{cm})^2$. To fit the SSH observation, 3D-Var produces T and S increments with largest amplitude at the level of the thermocline. The vertical structures are noticeably anisotropic. The increments display a pronounced upward tilt from west to east commensurate with the tilt of the background isotherms in this region. This anisotropic response is produced by the gradient-dependent T variances. The S increment has a dipole-like structure where the transition from negative to positive values occurs at the level of the salinity maximum in the background state. Above this level, the vertical derivative of the background salinity is negative (salinity increases with depth), whereas below this level, the vertical derivative is positive (salinity decreases with depth). Since the vertical derivative of the background temperature is everywhere negative (temperature decreases with depth), there is a change in sign in the derivative $\partial S/\partial T|_{T=T^b,S=S^b}$ in (17) which gives rise to the dipole in Fig. 3b.

The previous examples illustrate the fundamental importance of the balance operator in establishing a physically sensible (multivariate) response in 3D-Var. The balance operator also plays an important role in 4D-Var. This is illustrated in Fig. 4 which shows the SSH increments produced from two 4D-Var single T observation experiments performed without and with the balance operator activated (Figs. 4a and b, respectively). The geographical location of the single T observation is the same as in the example in Fig. 2. In these experiments, the control variables are a function of the model initial conditions which are taken to be 10 days before the observation time. For the experiment without the balance operator, the background-error covariances must be specified for the full fields at initial time. The correlation models for S and velocity are taken to be identical to those used by Weaver *et al.* (2003) for a rigid-lid version of OPA, while the correlation model for SSH is taken to be identical to the horizontal correlation model for T and S. The variances are set to values typical of the climatological variability of these fields: $(0.08\,\mathrm{m})^2$ for SSH, and surface values of $(0.25\,\mathrm{psu})^2$ for S, $(0.4\,\mathrm{m/s})^2$ for u, and $(0.1\,\mathrm{m/s})^2$ for v. The variances for S, u and v are gradually reduced below the surface. For the experiment with the balance operator, the unbalanced variances are set to zero as in the previous example, while the variances of the balanced components are defined implicitly via interactions between the balance operator and univariate T covariances.

The increments shown in Figs. 4a and b are those produced at the observation time (day 10) and have been computed by using the tangent-linear model to propagate forward the analysis increment at initial time. The SSH increment in the first 4D-Var experiment has localized structure similar to that obtained by 3D-Var with

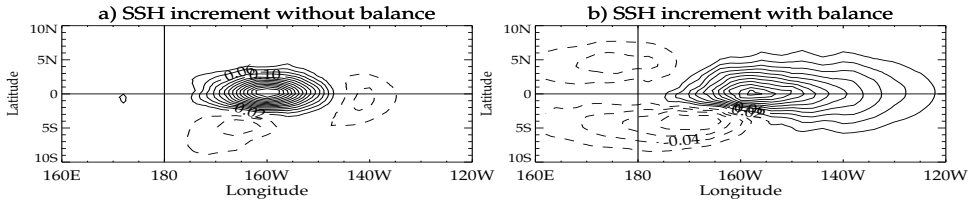

Figure 4: Horizontal section of the SSH analysis increments generated by the 4D-Var assimilation of a single temperature observation (positive innovation) located 10 days into an assimilation window at the same geographical location as in the example in Fig. 2. The increments are displayed on day 10 for a 4D-Var experiment a) without and b) with the balance operator activated. The fields have been multiplied by a factor 100 and the same contour interval has been used in panels a) and b), and Fig. 2e. Solid (dashed) contours indicate positive (negative) values.

the balance operator (cf. Fig. 4a and Fig. 2e). In terms of the analysis of SSH, nothing much appears to have been gained by using 4D-Var. When the balance operator is included, however, the temperature observation projects much more effectively onto large-scale equatorial wave-modes as clearly illustrated in Fig. 4b by the presence of a westward-propagating baroclinic Rossby wave to the west of the observation location. Contrary to the 4D-Var experiment without the balance operator, the observation is able to have a much wider impact than in 3D-Var.

5 Summary and conclusions

The background-error covariances are often cited as a critical component of a statistical data assimilation system. An arguably more fundamental component is the operator that is needed to compute the model counterpart of the assimilated observations. In this paper, it was shown how linear balance and smoothness constraints that are traditionally used to model multivariate covariances of background error could be cast within the more general, nonlinear, framework of an observation operator. The key aspect of this procedure is the design of a transformation, possibly nonlinear, from the space of highly correlated model state variables to a space of nondimensional control variables that are approximately mutually uncorrelated. In the space of the transformed variables, the background-error covariance matrix is assumed to be the identity matrix. The inverse of the transformation, or its generalized inverse if the dimension of the control space is smaller than that of model space, is also needed so not all transformations are suitable.

This paper outlined a control variable transformation for application to variational ocean data assimilation. The focus was on the balance operator, the inverse of which is designed to decorrelate the model state variables of temperature, salinity, SSH and velocity. In the proposed formulation, the inverse of the sequence of balance relationships left temperature unaltered but removed parts from salinity that could be related to temperature, parts from SSH that could be related to temperature and salinity, and parts from velocity that could be related to temperature, salinity and SSH. Both linear constraints (geostrophy, hydrostatic, dynamic height) and nonlinear constraints (T-S relationship, equation of state) were employed. In incremental variational assimilation, nonlinear constraints are linearized about a reference state as part of the minimization process. Furthermore, by linearizing the control variable transformation within the definition of the reference state itself, the minimization problem can be solved without the need to perform either the nonlinear transformation or its inverse. This is a convenient approximation but may break down when the increments are large. Further research is needed to quantify the impact of this approximation for the nonlinear balance operator proposed here.

Evidence that the proposed ocean balance operator can explain a substantial amount of actual background-error variance was provided by considering the statistical balance properties of a large set of differences between

model forecasts verifying at the same time. Single observation experiments were performed to illustrate the multivariate analysis structures implied by the balance operator. One example illustrated how the balance operator could be used as an effective way to project SSH (altimeter) data onto the subsurface density field in 3D-Var. Another example illustrated the potential benefits of the balance operator for equatorial analysis with 4D-Var. To obtain full benefit from the balance formulation in realistic implementations will require careful specification of the error covariance statistics of the transformed (uncorrelated) state variables. Ensemble methods could be very promising for this purpose.

Acknowledgements

This work is part of a collaboration between CERFACS and ECMWF to develop advanced ocean assimilation methods for climate research and seasonal forecasting. Support for this work was provided by the European ENACT project (contract No. EVK2-CT2001-00117) and the Groupe Mission MERCATOR / CORIOLIS. We are grateful to Magdalena Balmaseda for her suggestions for improving an earlier version of this report. This report also appears as a CERFACS Technical Report (TR/CMGC/06/16).

Appendix A: Matrix representation of the background-error covariance model

In this appendix, an explicit form of the background-error covariance matrix is derived to illustrate how, on a given outer iteration of the incremental variational algorithm (Eq. (10)), the components of the balance operator combine with the univariate blocks of the covariance matrix of the uncorrelated variables to produce a full-rank multivariate covariance matrix for the model variables. For clarity of notation, the superscript $k-1$ on linearized operators will be omitted. From (10), the background-error covariance matrix of the model state $\mathbf{x}$ is related to the background-error covariance matrix of the uncorrelated state variables $\widehat{\mathbf{x}}$ by

$$\mathbf{B}_{(\mathbf{x})} = \mathbf{K}\mathbf{B}_{(\widehat{\mathbf{x}})}\mathbf{K}^T \tag{28}$$

where $\mathbf{B}_{(\widehat{\mathbf{x}})} = \mathbf{D}_{(\widehat{\mathbf{x}})}\,\mathbf{F}\,\mathbf{F}^T\,\mathbf{D}^T_{(\widehat{\mathbf{x}})}$ is a block matrix of the form

$$\mathbf{B}_{(\widehat{\mathbf{x}})} = \begin{pmatrix} \mathbf{B}_{TT} & 0 & 0 & 0 & 0 \\ 0 & \mathbf{B}_{S_U S_U} & 0 & 0 & 0 \\ 0 & 0 & \mathbf{B}_{\eta_U \eta_U} & 0 & 0 \\ 0 & 0 & 0 & \mathbf{B}_{u_U u_U} & \mathbf{B}^T_{v_U u_U} \\ 0 & 0 & 0 & \mathbf{B}_{v_U u_U} & \mathbf{B}_{v_U v_U} \end{pmatrix}, \tag{29}$$

with $\mathbf{B}_{\widehat{x}\widehat{x}} = \mathbf{D}_{\widehat{x}}\mathbf{F}_{\widehat{x}\widehat{x}}\mathbf{F}^T_{\widehat{x}\widehat{x}}\mathbf{D}^T_{\widehat{x}}$, $\widehat{x} = T$, S_U, η_U and $\mathbf{u}^h_U$. The four-block submatrix in the lower corner of (29) corresponds to $\mathbf{B}_{\mathbf{u}^h_U\mathbf{u}^h_U}$. A non-zero cross-covariance between u_U and v_U arises since the smoothing operator $\mathbf{F}_{\mathbf{u}^h_U\mathbf{u}^h_U}$ employed involves a vector Laplacian operator which smooths separately horizontal divergence and relative vorticity (Weaver *et al.* 2003).

The balance operator is a lower diagonal matrix of the form

$$\mathbf{K} = \begin{pmatrix} \mathbf{I} & 0 & 0 & 0 & 0 \\ \mathbf{K}_{ST} & \mathbf{I} & 0 & 0 & 0 \\ \mathbf{K}_{\eta T} & \mathbf{K}_{\eta S} & \mathbf{I} & 0 & 0 \\ \mathbf{K}_{uT} & \mathbf{K}_{uS} & \mathbf{K}_{u\eta} & \mathbf{I} & 0 \\ \mathbf{K}_{vT} & \mathbf{K}_{vS} & \mathbf{K}_{v\eta} & 0 & \mathbf{I} \end{pmatrix} \tag{30}$$

where, from (15) and (16),

$$\begin{aligned}
\mathbf{K}_{\eta T} &= \mathbf{K}_{\eta\rho}\mathbf{K}_{\rho T} \\
\mathbf{K}_{uT} &= \mathbf{K}_{up}\mathbf{K}_{p\rho}\mathbf{K}_{\rho T} \\
\mathbf{K}_{vT} &= \mathbf{K}_{vp}\mathbf{K}_{p\rho}\mathbf{K}_{\rho T} \\
\mathbf{K}_{\eta S} &= \mathbf{K}_{\eta\rho}\mathbf{K}_{\rho S} \\
\mathbf{K}_{uS} &= \mathbf{K}_{up}\mathbf{K}_{p\rho}\mathbf{K}_{\rho S} \\
\mathbf{K}_{vS} &= \mathbf{K}_{vp}\mathbf{K}_{p\rho}\mathbf{K}_{\rho S} \\
\mathbf{K}_{u\eta} &= \mathbf{K}_{up}\mathbf{K}_{p\eta} \\
\mathbf{K}_{v\eta} &= \mathbf{K}_{vp}\mathbf{K}_{p\eta}.
\end{aligned}$$

Substituting (29) and (30) in (28) and carrying out the matrix multiplication gives

$$\mathbf{B}_{(\mathbf{x})} = \begin{pmatrix}
\mathbf{B}_{TT} & \mathbf{B}_{ST}^T & \mathbf{B}_{\eta T}^T & \mathbf{B}_{uT}^T & \mathbf{B}_{vT}^T \\
\mathbf{B}_{ST} & \mathbf{B}_{SS} & \mathbf{B}_{\eta S}^T & \mathbf{B}_{uS}^T & \mathbf{B}_{vS}^T \\
\mathbf{B}_{\eta T} & \mathbf{B}_{\eta S} & \mathbf{B}_{\eta\eta} & \mathbf{B}_{u\eta}^T & \mathbf{B}_{v\eta}^T \\
\mathbf{B}_{uT} & \mathbf{B}_{uS} & \mathbf{B}_{u\eta} & \mathbf{B}_{uu} & \mathbf{B}_{vu}^T \\
\mathbf{B}_{vT} & \mathbf{B}_{vS} & \mathbf{B}_{v\eta} & \mathbf{B}_{vu} & \mathbf{B}_{vv}
\end{pmatrix} \tag{31}$$

where

$$\begin{aligned}
\mathbf{B}_{ST} &= \mathbf{K}_{ST}\mathbf{B}_{TT} \\
\mathbf{B}_{\eta T} &= \mathbf{K}_{\eta T}\mathbf{B}_{TT} \\
\mathbf{B}_{uT} &= \mathbf{K}_{uT}\mathbf{B}_{TT} \\
\mathbf{B}_{vT} &= \mathbf{K}_{vT}\mathbf{B}_{TT} \\
\mathbf{B}_{SS} &= \mathbf{K}_{ST}\mathbf{B}_{TT}\mathbf{K}_{ST}^T + \mathbf{B}_{S_US_U} \\
\mathbf{B}_{\eta S} &= \mathbf{K}_{\eta T}\mathbf{B}_{TT}\mathbf{K}_{ST}^T + \mathbf{K}_{\eta S}\mathbf{B}_{S_US_U} \\
\mathbf{B}_{uS} &= \mathbf{K}_{uT}\mathbf{B}_{TT}\mathbf{K}_{ST}^T + \mathbf{K}_{uS}\mathbf{B}_{S_US_U} \\
\mathbf{B}_{vS} &= \mathbf{K}_{vT}\mathbf{B}_{TT}\mathbf{K}_{ST}^T + \mathbf{K}_{vS}\mathbf{B}_{S_US_U} \\
\mathbf{B}_{\eta\eta} &= \mathbf{K}_{\eta T}\mathbf{B}_{TT}\mathbf{K}_{\eta T}^T + \mathbf{K}_{\eta S}\mathbf{B}_{S_US_U}\mathbf{K}_{\eta S}^T + \mathbf{B}_{\eta_U\eta_U} \\
\mathbf{B}_{u\eta} &= \mathbf{K}_{uT}\mathbf{B}_{TT}\mathbf{K}_{\eta T}^T + \mathbf{K}_{uS}\mathbf{B}_{S_US_U}\mathbf{K}_{\eta S}^T + \mathbf{K}_{u\eta}\mathbf{B}_{\eta_U\eta_U} \\
\mathbf{B}_{v\eta} &= \mathbf{K}_{vT}\mathbf{B}_{TT}\mathbf{K}_{\eta T}^T + \mathbf{K}_{vS}\mathbf{B}_{S_US_U}\mathbf{K}_{\eta S}^T + \mathbf{K}_{v\eta}\mathbf{B}_{\eta_U\eta_U} \\
\mathbf{B}_{uu} &= \mathbf{K}_{uT}\mathbf{B}_{TT}\mathbf{K}_{uT}^T + \mathbf{K}_{uS}\mathbf{B}_{S_US_U}\mathbf{K}_{uS}^T + \mathbf{K}_{u\eta}\mathbf{B}_{\eta_U\eta_U}\mathbf{K}_{u\eta}^T + \mathbf{B}_{u_Uu_U} \\
\mathbf{B}_{vu} &= \mathbf{K}_{vT}\mathbf{B}_{TT}\mathbf{K}_{uT}^T + \mathbf{K}_{vS}\mathbf{B}_{S_US_U}\mathbf{K}_{uS}^T + \mathbf{K}_{v\eta}\mathbf{B}_{\eta_U\eta_U}\mathbf{K}_{u\eta}^T + \mathbf{B}_{v_Uu_U} \\
\mathbf{B}_{vv} &= \mathbf{K}_{vT}\mathbf{B}_{TT}\mathbf{K}_{vT}^T + \mathbf{K}_{vS}\mathbf{B}_{S_US_U}\mathbf{K}_{vS}^T + \mathbf{K}_{v\eta}\mathbf{B}_{\eta_U\eta_U}\mathbf{K}_{v\eta}^T + \mathbf{B}_{v_Uv_U}.
\end{aligned}$$

To interpret the results of the single observation experiments in section 4, it is helpful to illustrate how the algebraic structure of (31) determines the expression for the increment $\delta\mathbf{x}^k$ on each outer iteration. Consider the exact minimizing solution of (4), which is found by setting the gradient of (4) to zero and solving for $\delta\mathbf{v}^k$ (e.g., see Daley 1991):

$$\delta\mathbf{v}^k = \mathbf{G}^T\left(\mathbf{G}\mathbf{G}^T + \mathbf{R}\right)^{-1}\mathbf{d}^{o,k}. \tag{32}$$

For a single observation, $\mathbf{d}^{o,k} = d^{o,k}$, $\mathbf{R} = (\sigma^o)^2$ and $\mathbf{G}\mathbf{G}^T = (\sigma^k)^2$ are scalars, where the latter two quantities correspond to, respectively, the observation-error variance and the effective background-error variance for the observation on the k-th outer iteration. If the observation is situated at the end of the assimilation window ($t = t_n$) then $\mathbf{G} = \mathbf{H}_n\mathbf{M}(t_n,t_0)\mathbf{U}$ where $\mathbf{H}_n = \mathbf{h}^T$ is the observation operator, which for a single observation is a vector of the same length as $\delta\mathbf{x}$, and $\mathbf{M}(t_n,t_0)$ is the linearized forward propagator which is the identity matrix in 3D-Var (FGAT) and the tangent-linear operator in 4D-Var. Substituting these expressions into (32) and transforming the increment into model space gives

$$\delta\mathbf{x}^k = \mathbf{U}\,\delta\mathbf{v}^k = c\,\mathbf{B}_{(\mathbf{x})}\,\mathbf{M}(t_n,t_0)^T\,\mathbf{h} \tag{33}$$

where $c = d^{o,k}\,[(\sigma^k)^2 + (\sigma^o)^2]^{-1}$ and, from (10), $\mathbf{B}_{(\mathbf{x})} = \mathbf{U}\mathbf{U}^T$. From (33) it is clear that $\delta\mathbf{x}^k$ will be proportional to the columns of the matrix $\mathbf{B}_{(\mathbf{x})}\mathbf{M}(t_n,t_0)^T$, or simply the columns of $\mathbf{B}_{(\mathbf{x})}$ in the case of 3D-Var. For example, for a temperature observation $\mathbf{h} = (\mathbf{e}^T,0,0,0,0)^T$ where $\mathbf{e}$ is a vector corresponding to the temperature components of $\delta\mathbf{x}^k$, and the other elements of $\mathbf{h}$ are zero vectors corresponding to the other variable components. (If the temperature observation is located exactly at a model grid point then $\mathbf{e} = (0,...,0,1,0,...,0)^T$ where the non-zero entry is associated with that grid-point.) In this case, it is easy to see that the 3D-Var increment will be proportional to the first block-column of $\mathbf{B}_{(\mathbf{x})}$, in particular, dependent on $\mathbf{B}_{TT}$ and the forward balance operators only. Likewise, the 3D-Var increment will be proportional to the second block-column of $\mathbf{B}_{(\mathbf{x})}$ for a salinity observation, proportional to the third block-column of $\mathbf{B}_{(\mathbf{x})}$ for a SSH observation, and proportional to the third plus fourth block-columns of $\mathbf{B}_{(\mathbf{x})}$ for a velocity observation. Notice that in 4D-Var, regardless of what type of observation is assimilated, $\delta\mathbf{x}^k$ will be a non-trivial linear combination of all block-columns of $\mathbf{B}_{(\mathbf{x})}$ since the action of the adjoint operator $\mathbf{M}(t_n,t_0)^T$ will result in a transfer of information from the observed quantity to all model variables.

REFERENCES

Alves, O., Alonso-Balmaseda, M., Anderson, D. L. T. and Stockdale, T., 2004: Sensitivity to dynamical seasonal forecasts to ocean initial conditions. *Q. J. R. Meteorol. Soc.*, **130**, 647–668.

Balmaseda, M. A., 2004 'Ocean data assimilation for seasonal forecasts'. Pp. 301–325 in Proceedings of the ECMWF Seminar on Recent Developments in data assimilation for atmosphere and ocean, 8-12 September 2003, Reading, England.

Behringer, D., Ji, M. and Leetma, A., 1998: An improved coupled model for ENSO prediction and implications for ocean initialization. Part I: The ocean data assimilation system. *Mon. Wea. Rev.*, **126**, 1013–1021.

Bennett, A. F., Chua, B. S., Harrison, D. E. and McPhaden, M. J., 2000: Generalized inversion of Tropical Atmosphere-Ocean (TAO) data using a coupled model of the tropical Pacific. *J. Climate*, **13**, 2770–2785.

Berre, L., Ştefănescu, S. E. and Pereira, M. B., 2005: A comparison between an analysis ensemble approach and two other error simulation methods. *To appear in Tellus*.

Buehner, M., 2005: Ensemble-derived stationary and flow-dependent background-error covariances: Evaluation in a quasi-operational NWP setting. *Q. J. R. Meteorol. Soc.*, **131**, 1013–1044.

Burgers, G., Balmaseda, M. A., Vossepoel, F. C., van Oldenborgh, G. J. and van Leeuwen, P. J., 2002: Balanced ocean-data assimilation near the equator. *J. Phys. Oceanogr.*, **32**, 2509-2519.

Courtier, P., Thépaut, J.-N. and Hollingsworth, A., 1994: A strategy for operational implementation of 4D-Var, using an incremental approach. *Q. J. R. Meteorol. Soc.*, **120**, 1367–1388.

Cullen, M. J. P., 2003: Four-dimensional variational data assimilation: A new formulation of the background-error covariance matrix based on a potential-vorticity representation. *Q. J. R. Meteorol. Soc.*, **129**, 2777–2796.

Daley, R., 1991: *Atmospheric data analysis.* Cambridge atmospheric and space sciences series, Cambridge University Press.

Derber, J. and Wu, W.-S., 1998: The use of TOVS cloud-cleared radiances in the NCEP SSI analysis system. *Mon. Wea. Rev.*, **126**, 2287–2299.

Derber, J. and Bouttier, F., 1999: A reformulation of the background error covariance in the ECMWF global data assimilation system. *Tellus*, **51A**, 195–221.

Ferry, N., 2003: Assimilation et surface libre dans les modèles océaniques MERCATOR. Rapport interne Projet MERCATOR, Référence MOO-ST-410-231-MER.

Fukumori, I., Raghunath, R. and Fu, L., 1998: Nature of global large-scale sea level variability in relation to atmospheric forcing: a modeling study. *J. Geophys. Res.*, **103**, 5493–5512.

Golub, G. and Van Loan, C. F., 1996: *Matrix Computations.* The Johns Hopkins University Presss, London.

Han, G., Zhu, J. and Zhou, G., 2004: Salinity estimation using the T-S relation in the context of variational data assimilation. *J. Geophys. Res.*, **109**, C03018, doi:10.1029/2003JC001781.

Ingleby, B. and Huddleston, M., 2005: Quality control of ocean temperature and salinity profiles - historical and real-time data. *To appear in J. Mar. Sys.*.

Keppenne, C. L. and Rienecker, M. M., 2003: Assimilation of temperature into an isopycnal ocean general circulation model using a parallel ensemble Kalman filter. *J. Mar. Sys.*, **40-41**, 363–380.

Lagerloef, G. S. E., Mitchum, G. T., Lukas, R. B. and Niiler, P. P., 1999: Tropical Pacific near-surface currents estimated from altimeter, wind, and drifter data. *J. Geophys. Res.*, **104**, 23313–23326.

Lermusiaux, P. F. J., Anderson, D. G. M. and Lozano, C. J., 2000: On the mapping of multivariate geophysical fields: error and variability subspace estimates. *Q. J. R. Meteorol. Soc.*, **126**, 1387–1430.

Lorenc, A. C., 2003: Modelling of error covariances by 4D-Var data assimilation. *Q. J. R. Meteorol. Soc.*, **129**, 3167–3182.

Madec, G., Delecluse, P., Imbard, M. and Levy, C., 1998: OPA 8.1 Ocean General Circulation Model Reference Manual. Technical note no. 11, LODYC/IPSL, Paris, France.

McDougall, T. J., Jackett, D. R., Wright, D. G. and Feistel, R., 2003: Accurate and computationally efficient algorithms for potential temperature and density of seawater. *J. Atmos. Ocean. Technol.*, **20**, 730–741.

Parrish, D. F. and Derber, J. C., 1992: The National Meteorological Center's spectral statistical interpolation analysis system. *Mon. Wea. Rev.*, **120**, 1747–1763.

Picaut, J. and Tournier, R., 1991: Monitoring the 1979-1985 equatorial Pacific current transports with expendable bathythermograph data. *J. Geophys. Res.*, **96**, 3263–3277.

Ricci, S., Weaver, A. T., Vialard, J. and Rogel, P., 2005: Incorporating temperature-salinity constraints in the background error covariance of variational ocean data assimilation. *Mon. Wea. Rev.*, **133**, 317–338.

Roullet, G. and Madec, G., 2000: Salt conservation, free surface, and varying levels: a new formulation for ocean general circulation models. *J. Geophys. Res.*, **105**, 23927–23942.

Stammer, D., Wunsch, C., Giering, R., Eckert, C., Heimbach, P., Marotzke, J., Adcroft, A., Hill, C. N. and Marshall, J., 2002: Global ocean circulation during 1992-1997, estimate from ocean observations and a general

circulation model. *J. Geophys. Res.*, **107**, C93118, doi:10.1029/2001JC000888.

Testut, C.-E., Brasseur, P., Brankart, J. M. and Verron, J., 2003: Assimilation of sea-surface temperature and altimetric observations during 1992-1993 into an eddy permitting primitive equation model of the North Atlantic Ocean. *J. Mar. Sys.*, **40-41**, 291–316.

Troccoli, A. and Haines, K., 1999: Use of Temperature-Salinity relation in a data assimilation context. *J. Atmos. Ocean. Technol.*, **16**, 2011–2025.

Troccoli, A., Alonso Balmaseda, M., Segschneider, J., Vialard, J., Anderson, D. L. T., Stockdale, T., Haines, K. and Fox, A. D., 2002: Salinity adjustments in the presence of temperature data assimilation. *Mon. Wea. Rev.*, **130**, 89–102.

Uppala, S. M. and Co-authors, 2005: The ERA-40 re-analysis. *Q. J. R. Meteorol. Soc.*, **131**, 2961–3012.

Weaver, A. T., Vialard, J. and Anderson, D. L. T., 2003: Three- and four-dimensional variational assimilation with an ocean general circulation model of the tropical Pacific Ocean. Part 1: formulation, internal diagnostics and consistency checks. *Mon. Wea. Rev.*, **131**, 1360–1378.

Weaver, A. T. and Courtier, P., 2001: Correlation modelling on the sphere using a generalized diffusion equation. *Q. J. R. Meteorol. Soc.*, **127**, 1815–1846.